A Numerical Study to Investigate the Hydrodynamic Properties of Nanowire Motion in Liquid

S Özer*

Department of Biomedical Engineering, İstanbul Yeniyuzyil University, 34100 İstanbul, Turkey

ABSTRACT

Manipulating micro(nano)-sized entities in liquid environment is a challenging yet necessary task in nanoscience and nanotechnology development. Due to the small dimensions, viscous behavior dominates the micro(nano)-sized objects motion. In this study, a computational fluid dynamic (CFD) approach has been used to investigate hydrodynamic effects on a nanowire (NM) translating an rotating about its long and short axis. Several numerical methods dealing with solid motion in fluid, including some CFD methods and Finite element analysis (FEA), have been compared. The change in drag coefficient with NW length, NW diameter, translational velocity, rotation speed, and wall effects has been researched. As a model, nanowires with 1-10 μm dimensions and 50 nm-250 nm diameters were investigated in liquid, with velocities of 0.5-500 μm/s. Nanowire is rotated about its long axis with an angular velocity of $\omega=0.25\pi$, 0.5π, 1.0π, 2.0π rad/s, and about its short axis with a fluid flow allow the rotation of the nanowire whose one end is constrained to a rotational motion around x and y axis. These models were also compared with the existing analytical models. Good agreement was observed between the numerical results and analytical calculations. The FEA model is also repeated in the closed boundary to investigate the wall effects on the nanowire's motion in liquid environment.

1. INTRODUCTION

Nanoscale manipulation is of tremendous importance in the application of nanowire-based devices like chemical and biological sensors, light-emitting diodes, and field effect transistors, magnetic tweezers, optical tweezers, microrobotics systems [1-7]. Accurate control and manipulate nanoscale objects can be helpful for nanoscience and nanotechnology. However, manipulation of such small objects is challenging, because van der Waals forces and other surface forces dominate gravitational forces and other volume forces at this scale [8]. One way to reduce these force effects is to perform the manipulation in liquid. Previously, it has been found that nanowires could be aligned or rotated by external magnetic or electrical field in liquid [9-15], however, the influence of the boundary conditions of nanowires in liquid were rarely taken into account, which can significantly affect the locomotion as they are close to a wall. In order to understand the manipulation of micron(nano)-sized materials in the liquid, it is necessary to fully understand the hydrodynamic forces acting on them. Measuring drag force on such a submicron scale bodies is challenging, and a problem of fundamental interest for microfluidic and molecular dynamics researchers [16]. From the theoretical viewpoint, it

_____

*Corresponding Author: sevilozer81@gmail.com

is still uncertain as to whether flow at this scale can be predicted by the Navier–Stokes equations solved for creeping conditions, solutions for which have been known since the end of the 19th century [17]. Experiments supported predictions down to Reynolds numbers <0.1, but the length scales investigated were many hundreds of nanometers [18].

   In this paper, we focus on nanowire translation parallel to its long axis, and rotational motion about its long and short axis in water. For this purpose, the hydrodynamic forces have been calculated for certain geometries such immersed nanowires moving through viscous fluids as they approach a surface at low Reynolds number. The model was also compared with the existing analytical models based on simple geometry and defined nanowires with common boundary conditions set for the liquid environment. Good agreement was observed between the numerical results and analytical calculations. The calculation is also repeated in a closed boundary to investigate the wall effect on the drag coefficient. If simplified nanowire as long slender cylinder, some analysis resolution had reported, such as cylinder rotating around long axis, translating along and against long axis [19-21]. But cylinder rotated around mid-point had no analysis resolution [22-23]. On a study, cylinder is divided into several sections, and simplified each section as little sphere, using the resolution fluid flowed around a sphere and relationship between each moving sphere, to obtain cylinder resisting model [24]. Another study simplified cylinder as several little section, to obtain fluid resisting model by considering the symmetry of cylinder [25]. All these models based on ellipsoid/cylinder translating could estimate nanowire resisting force and drag coefficient by external force driven [26]. There is another study which aims to investigate the drag force of unsmooth conical micromotors by using the normalization method [27].

2. THEORY AND NUMERICAL MODELLING WITH RESULTS

This part summarizes modeling efforts to predict hydrodynamic drag force imposed on an immersed nanowire due to its motion in viscous liquid. Finite element method (FEM) based models are developed for different boundary conditions to understand the effect of liquid cell geometry on hydrodynamics. Also, relevant analytical models are compared with FEM results.

2.1. Hydrodynamic Drag on Nanowires: Translational Motion Parallel to Long Axis

A finite element method-based model has been developed to analyze hydrodynamic drag force for nanowires in various geometries. The model is capable of simulating the behavior of a nanowire restricted to translational motion parallel to its long axis. The fluid flow due to an oscillating body at small amplitude requires the solution of the unsteady simplified Navier-Stokes equations for incompressible fluids:

$$\rho \frac{\partial U}{\partial t} = -\nabla P + \mu \nabla^2 U \rho \frac{\partial U}{\partial t}, \qquad \nabla . U = 0 \qquad (1)$$

where ρ and μ are the fluid density and viscosity. U and P are the fluid velocity and pressure, respectively. For the case of a nanowire, cylindrical coordinates can be used due to the symmetry conditions. Commercial finite element analysis software packages with fluid-structure interaction capabilities can be used to solve these equations for the immersed probes with complex geometries and boundary conditions. FEM software COMSOL handles this type of problems using Arbitrary Lagrangian-Eulerian (ALE) algorithm. Fluid-structure interaction (FSI) problems require the solution for the deformation of structures in fluid flow, which in

turn affects the flow pattern. COMSOL's ALE method handles the deforming geometries and the moving boundaries with a moving mesh grid.

Fig. 1 shows the computational domain for the simulations. Density and dynamic viscosity of the water are $1000\ kg/m^3$ and $1.0E-3\ Pa.$, respectively. Mechanical properties for the nanowire are initialized for that of Co with Young's modulus, E=110 GPa, Poisson's ratio, $v = 0.35$, thermal expansion coefficient, CTE: 17 µm/m. K, and Density, $d = 8700\ kg/m^3$
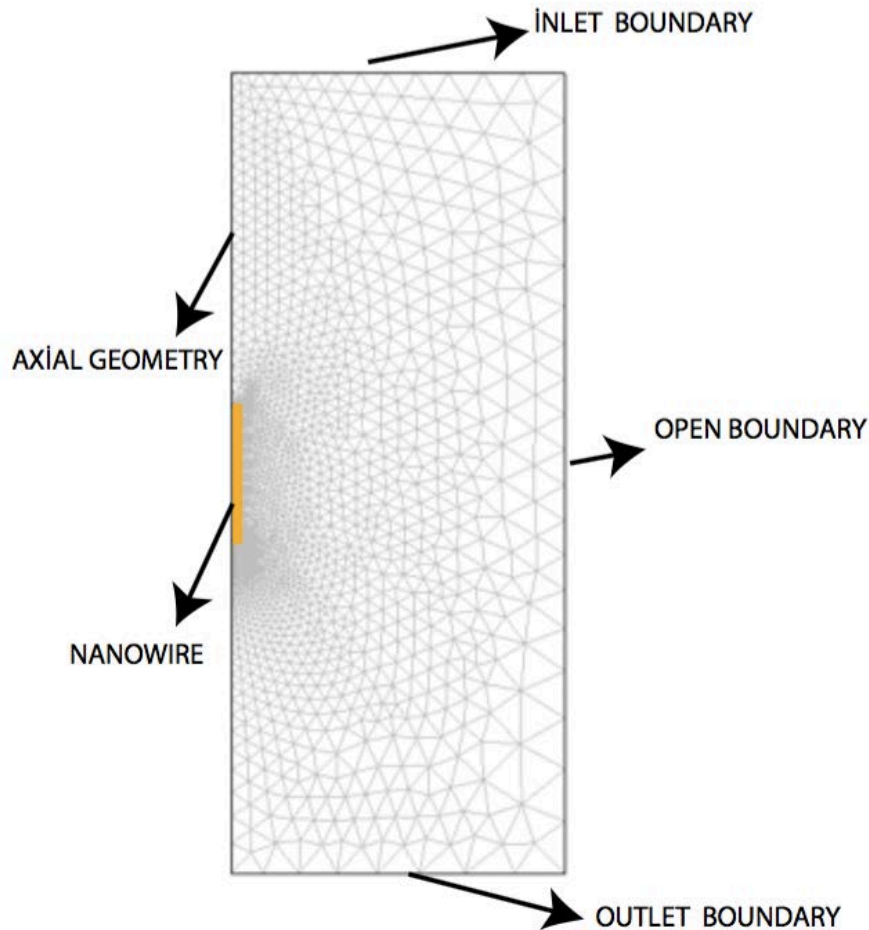
Fig. 1. Axisymmetric computational domain for an immersed nanowire. COMSOL Multiphysics: Fluid-Structure interaction (Incompressible Navier Stokes, Moving Mesh ALE, Axial Symmetry-stress/strain) module.

Individual computational domains have been created for nanowires with radii varying from 25 nm to 250 nm and lengths varying from 1 µm to 10 µm. Hydrodynamic drag affecting an immersed nanowire is evaluated by exposing the nanowire to a constant flow velocity imposed on the inlet port of the model. The velocity distribution in the volume is generated,

and the drag force of the nanowire is calculated using relevant post-processing tools. Velocity distribution for a model including a nanowire with a diameter of 200 nm and length of 10 µm is plotted in Fig. 2. Velocity field is normalized to the inlet velocity that is perpendicular to inlet port. The model is sensitive to the geometry of the containing fluid and the dimensions of the computational domain has been optimized separately for different nanowire geometries.
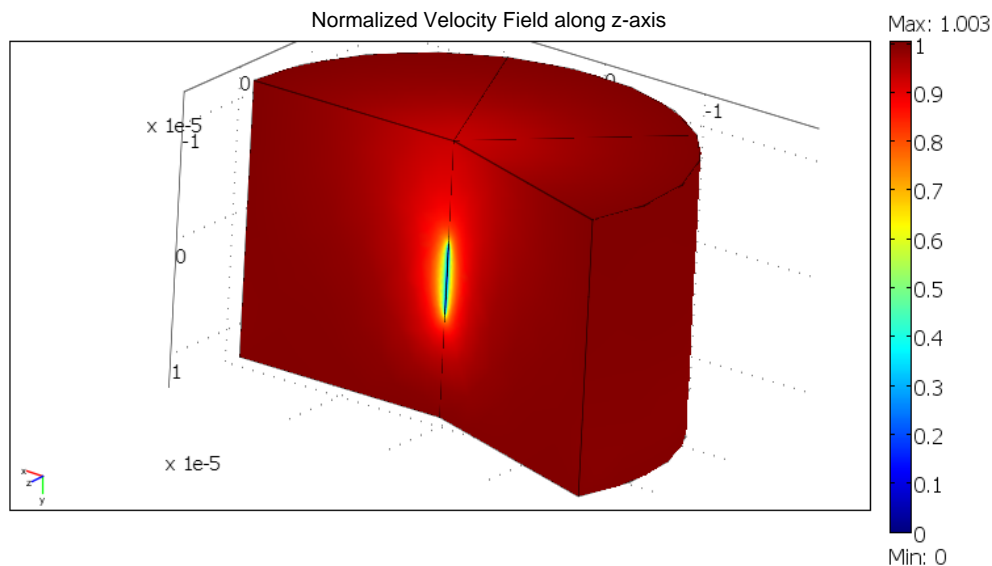

Fig. 2. Velocity distribution along y-axis for a model including a nanowire with a diameter of 200 nm and length of 10 µm.

2.2. Nanowires in Infinitely Large Liquid Medium

Hydrodynamic drag force (F) scales linearly with velocity imposed on the nanowire (U), so the ratio F/U can be defined as drag coefficient to compare the behavior of different nanowires. Drag coefficients for nanowires with radii varying from 25 nm to 250 nm and lengths varying from 1 µm to 10 µm are calculated through individual simulations. The dependence of drag coefficient on the length and diameter of a circular nanowire is shown in Fig. 3. The simulations were run for a rather slow velocity of 1×10^{-12} m/s to guarantee convergence of results without distorting moving mesh conditions. The results were cross-checked for velocity dependence and linear dependency between force and velocity was confirmed.

The results of FEM simulations are compared with approximate analytical models presented by Happel & Brenner [19] and Dupont [20]. Happel & Brenner solution is based on low Reynolds hydrodynamics and valid for circular cylinders. The drag force a cylinder moving its long axis is given by Eqn. 2:

$$\frac{F}{U} = \frac{8\pi\mu c}{((\tau^2+1).acoth(\tau)-\tau)} \tag{2}$$

where $\tau = {a}/{c}$, and $c = \sqrt{a^2 - b^2}$. $L = 2a$ is the length and $D = 2b$ is the diameter of a circular cylinder.

Dhont model based on a rod-like particle moving its long axis is given by Eqn 3:

$$\frac{F}{U} = \frac{2\pi\mu L}{\log{^L/_D}}$$ (3)

Drag coefficients for nanowires with diameters varying from 20 nm to 200 nm, and lengths varying from 1 μm to 20 μm are calculated as shown in Fig .4a-b. Dhont model is not valid for L ≈ D as can be noted, nevertheless, there is good agreement between different models. The calculations based on Happel & Brenner indicate that a drag force of 1.5 pN will be imposed on a nanowire with a length of 10 μm and a diameter of 200 nm. For the same geometry increases slightly to 1.6 pN for the model of Dhont.
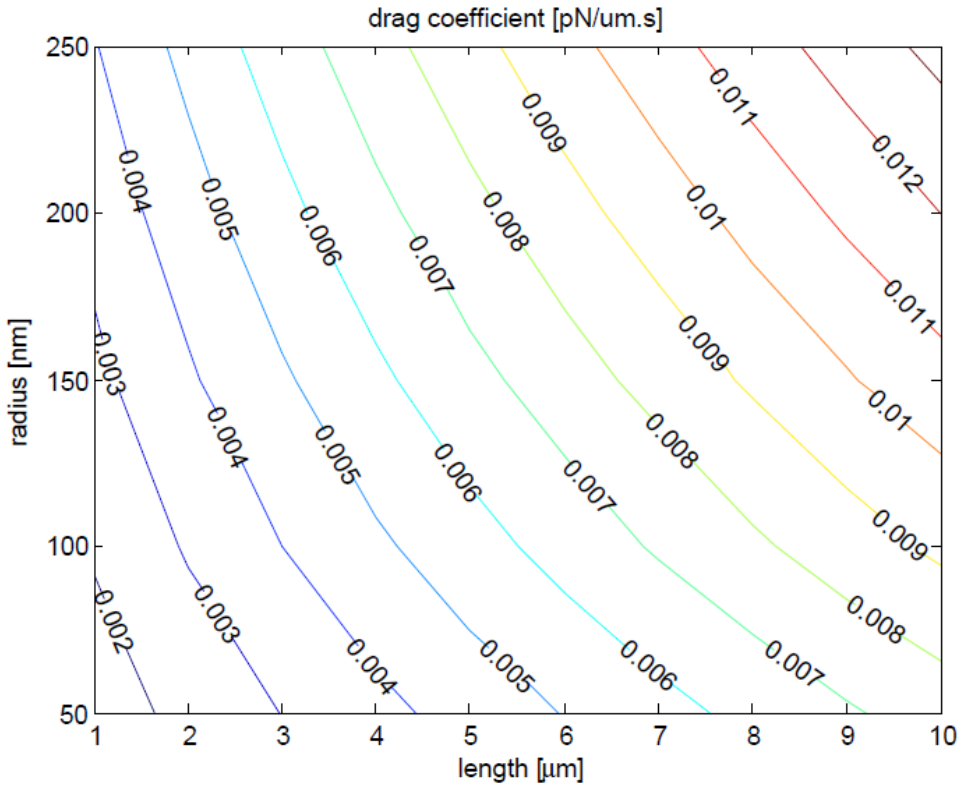

Fig. 3. The dependence of drag coefficient, i.e., ratio of drag force to velocity, on the length and diameter of a circular nanowire. Each of the data points corresponds to an individual FEM simulation.
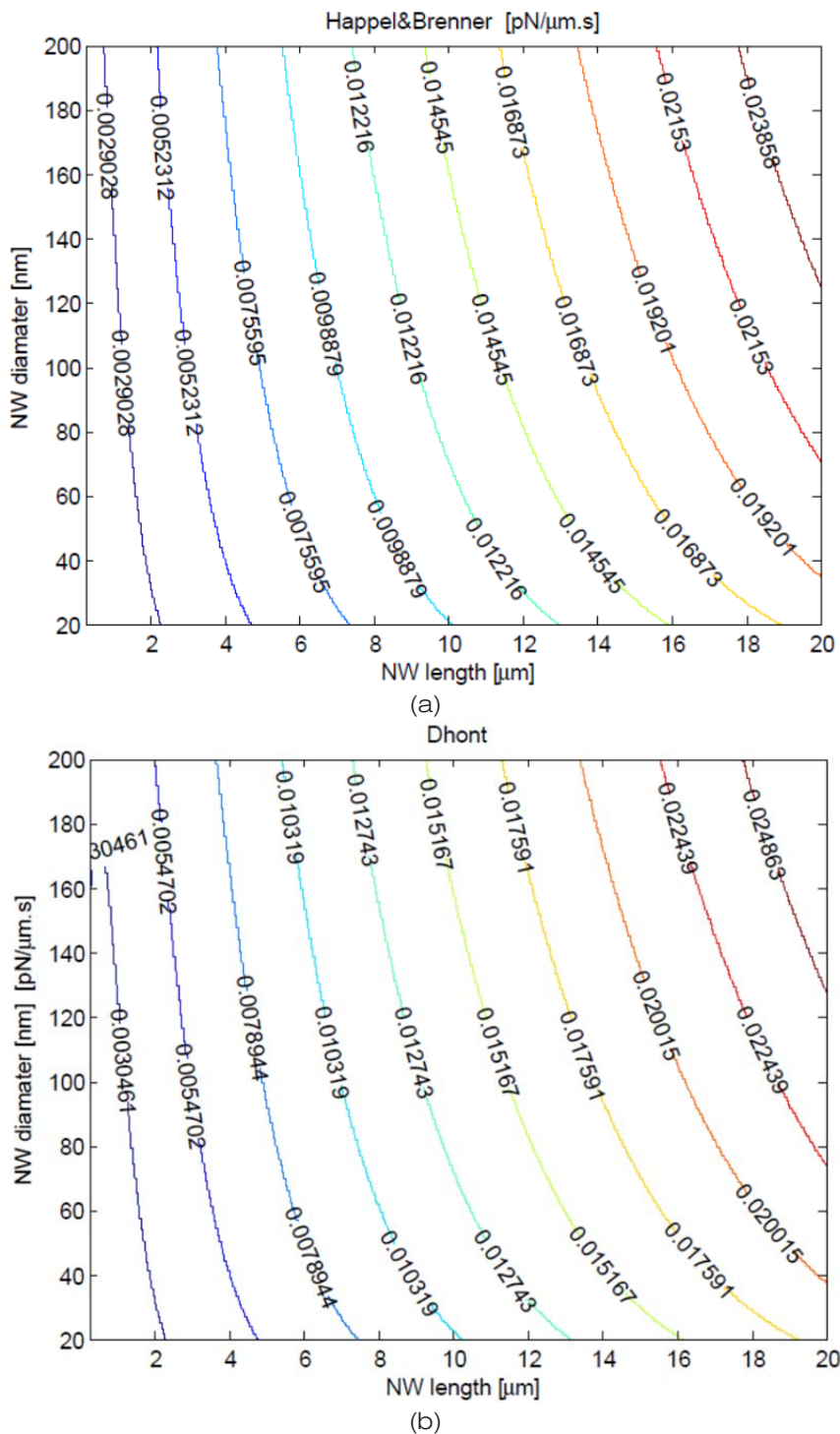
Fig. 4. The dependence of drag coefficient, i.e., ratio of drag force to velocity, on
the length and diameter of a circular nanowire, calculated using analytical models
presented by (a) Happel & Brenner [19], (b) Dhont [20].

2.3. Immersed Nanowires in Closed Medium

The model with open boundaries captures well the behavior of nanowires immersed in an infinitely large liquid domain. Hydrodynamics of immersed structures is altered significantly when they are within close proximity of stationary walls. Wall effects are especially important for nanowires kept in a microfluidic channel. Fig. 5(a) shows a cylindrical structure moving inside another stationary cylinder with open bases. An approximate solution for this problem was presented before in [19]. The drag coefficient for the enclosed nanowire is given in Eqn 4.

$$\frac{F}{U} = \frac{2\pi\eta L\left(1 - [2b^2/(R^2\text{-}b^2)].[1\text{-}\left\{\frac{2b^2}{R^2\text{-}b^2}\right\}.\{\log (R/b)\}]\right)}{(R^2+b^2).\left\{log\left(\frac{R}{b}\right)-1\right\}.(R^2-b^2)} \tag{4}$$

An equivalent model incorporating an inlet and outlet port is shown in Fig. 5(b). Defining inlet and outlet ports is computationally favorable for an FSI-FEM implementation using ALE algorithm. An axisymmetric model is built in FEM software accordingly.
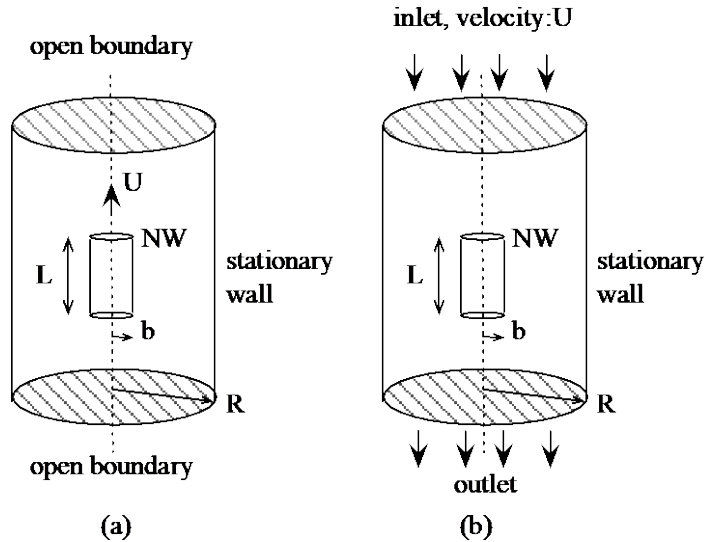

Fig. 5. (a) The model for a cylinder inside another cylinder. The model is adapted from ref. [19] to explain nanowire behavior. (b) The model for a cylinder inside another cylinder exposed to a uniform flow.

For a case study, drag coefficents are investigated for a nanowire with a radius of 250 nm and a length of 10 µm. The outer boundaries radius, R, is varied from 0.5 µm to 1000 µm. The inlet velocity is set to a small value, i.e., 10-12 m/s, to prevent mesh inversion problem. The dependence of the hydrodynamic drag on the fluid dimension can be seen in Fig. 6. The FEM results are compared with the approximation solution of cylindrical structure moving inside another stationary cylinder with open bases presented in [19]. There is a good agreement between the models suggesting that the drag coefficient increases significantly if the radius of

outer cylinder, R, is smaller than 40 µm for the chosen nanowire geometry. The variation of drag coefficient for R=40 µm and R=1 mm is only 10%. The findings can be generalized to any nanowire geometry. The drag coefficient is constant for practical purposes when ratio of outer cylinder length to nanowire length (or cylinder radius to nanowire radius) is larger than 5 (200) in this configuration (see Fig. 6).
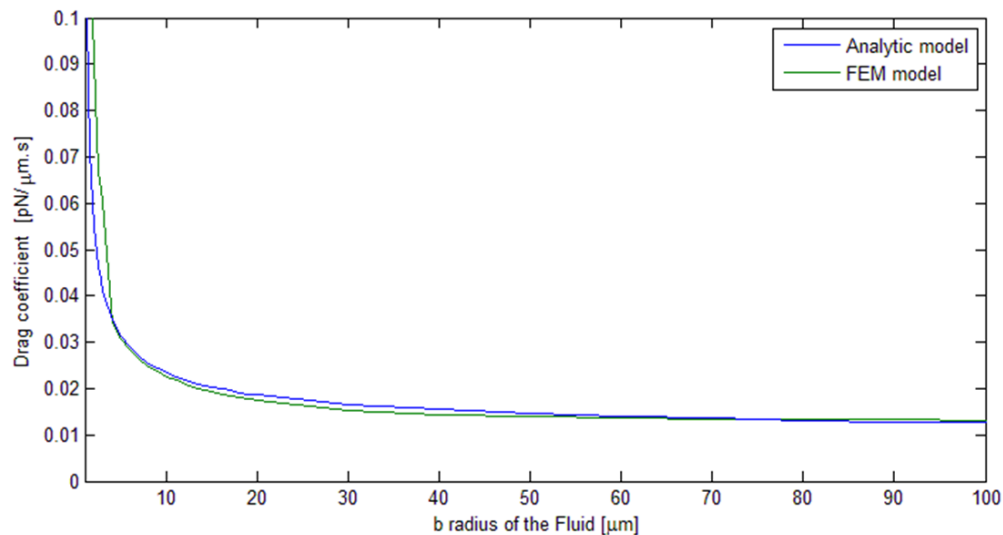

Fig. 6. FEM and analytical results for the drag coefficient for a circular cylinder moving inside another stationary cylinder with open bases as a function of radius of the outer cylinder, R.
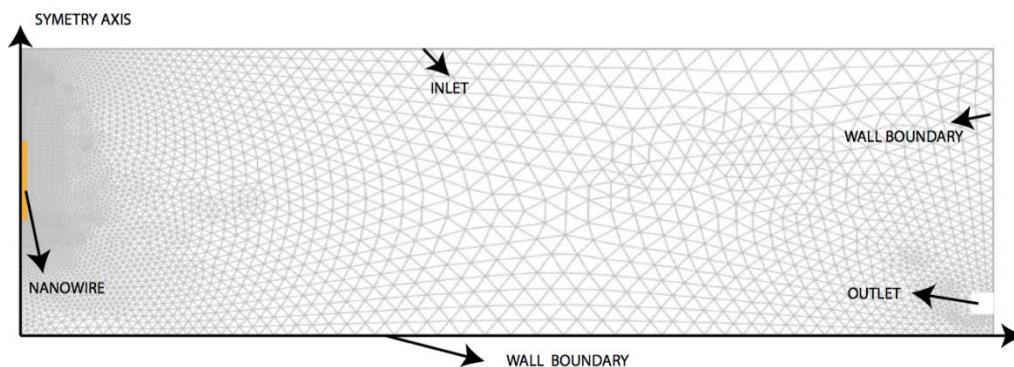

Fig. 7. Axisymmetric computational domain for a NW in a closed fluid cell. An auxiliary outlet is defined on the model for convergence of simulations successfully. The size and the location of the outlet is optimized so that its presence does not alter the results significantly.

The FEM model is verified using the approximate analytical model. The verified model is modified to study the hydrodynamics of nanowires in a completely enclosed chamber. The model with bottom edge assigned as a solid wall along with the side edge is shown in Fig. 7. An outlet port is still needed to have the simulations converge. Thus, a relatively small section is assigned as outlet with zero pressure. Ideally, the size and location of the outlet should not affect the results.

For different geometries of fluid domain, the outlet section is optimized in size and location so that the effect is limited in size to 15% and in location to 0.05%. Note that only the radius of the fluid is variable in fluid to get different geometries of fluid domain. For example, for a nanowire with a length of 10 µm and radius of 250 nm in a fluid domain of radius 250 µm and length of 100 µm, an outlet with a size of 1 µm is selected. The drag coefficients for NWs with different geometries in a closed fluid cell with a height of 100 µm and a radius of 250 µm is shown in Fig 8(a). The increase in drag coefficient when compared with the case when there are no stationary walls (comparing the results shown in Fig.3) is shown in Fig 8(b).

The models for the hydrodynamic drag force on the immersed nanowires are helpful for the design of nanowire geometries. The predicted drag force on a nanowire with a radius of 100 nm and a length of 10 µm that translates with a constant speed of 100 µm/s is around 1 pN and the drag force almost doubles when the nanowire is confined in a closed cylindrical liquid environment with a height of 100 µm and a radius of 250 µm. According to the simulation results the radius and the length of nanowires can be increased further without a substantial increase in drag force.
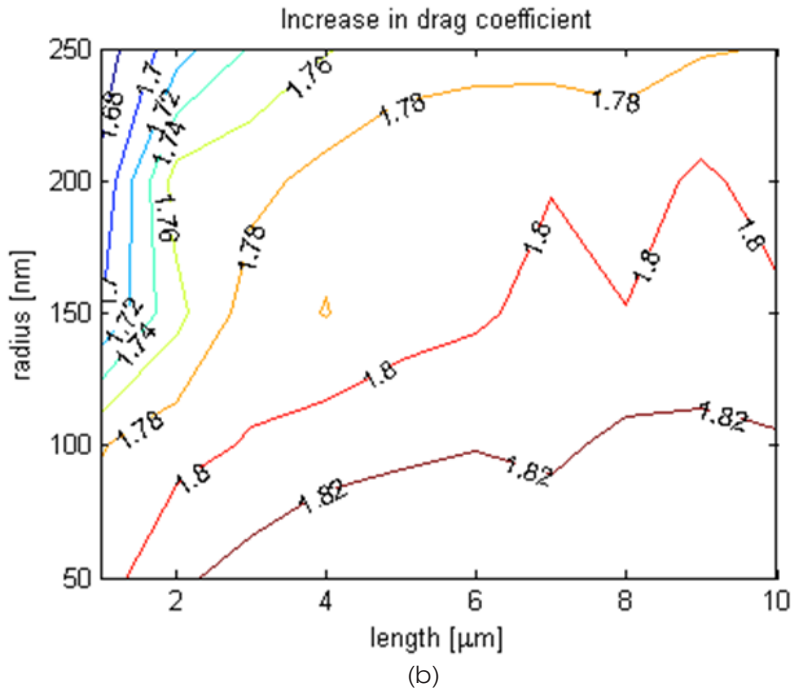

(a)

(b)
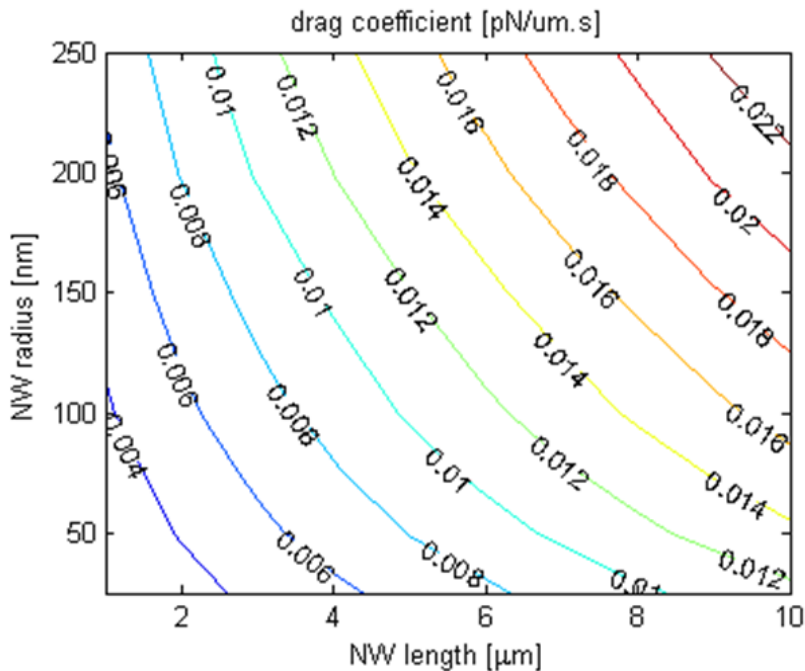
Fig. 8. (a) The dependence of drag coefficient, i.e., ratio of drag force to velocity, on the length and diameter of a circular nanowire in a closed fluid cell with a height of 100 µm and a radius of 250 µm. Each of the data points corresponds to an individual FEM simulation. (b) The increase in drag coefficient due to stationary walls for the selected geometry.

2.4. Nanowires in Rotational Motion about its long axis

In this part, hydrodynamic behavior of the nanowire in rotational motion about its long axis is examined. Cylindrical fluid domain is fixed to cylindrical dimension with 10 µm in radius and 50 µm in height. Nanowire is rotated about its long axis with an angular velocity of $\omega = 0.25 * pi, 0.5 * pi, 1.0 * pi, 2.0 * pi \ rad/s$ (Fig. 7). Due to the symmetry of the motion, 2 D Axisymmetric COMSOL Fluid Dynamics module is used for the analysis. Individual computational domains have been created for nanowires varying with radii from 25 nm to 250 nm and lengths varying from 1 µm to 10 µm. The boundaries of the computational domain in the model are defined as the wall (bottom) with no slip condition and the outlet ports (up/side) with zero pressure for the fluid domain, and as the sliding wall condition with a velocity of moving wall in ϕ direction for the nanowire. FEM simulations are also compared to an approximate analytical model. The relevant drag coefficient for a rod-like object is related to the rotation axes, and is given by the following Eqn. 5

$$\frac{\tau}{\omega} = \frac{\pi \eta L^3 (1+C)}{0.96 \ p^2} \tag{5}$$

For long axis rotation. Here, p=L/D, represents the length to diameter ratio, and C represents the end corrections for the rotational motion of the nanowire about its long axis. The value of the C is also calculated by the following Eqn. 6 [23] for the nanowire rotation about its long axis:

$$C = \frac{0.677}{p} - \frac{0.183}{p^2} \tag{6}$$

Fig. 9 compares the FEM simulations with the analytical model. about its long axis. For this computation, the nanowire diameter is fixed to 200 nm and the nanowire length has varied from 1 to 10 µm.
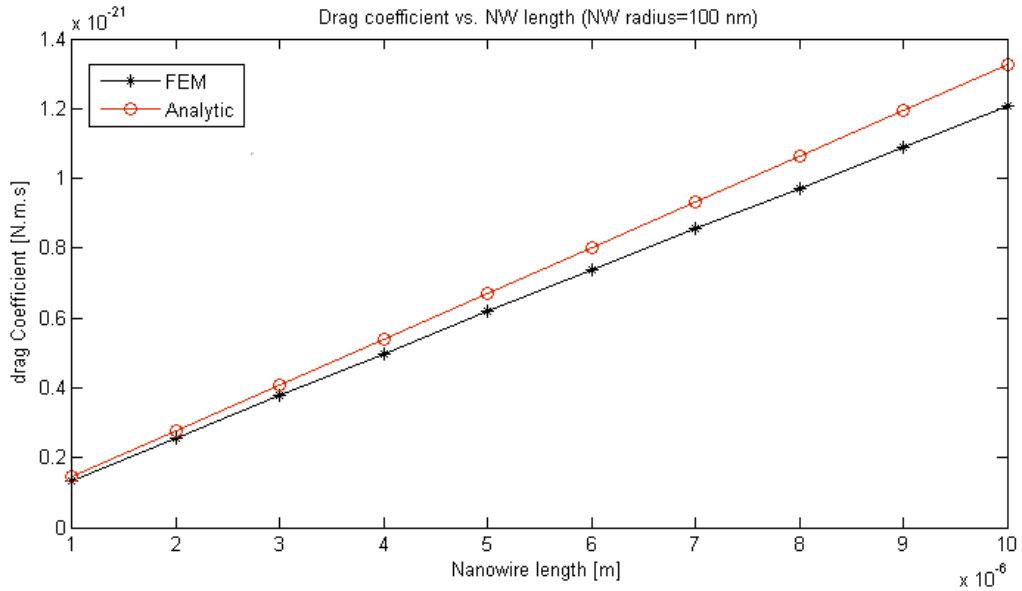

Fig. 9. The dependence of drag coefficient, i.e., ratio of torque to angular velocity, on the length of a circular nanowire. Each of the data points corresponds to an individual FEM simulation 2D-COMSOL Fluid Dynamics, Laminar flow module.

The dependence of the drag coefficient on the different nanowire diameters with a fixed 10 µm nanowire length is also compared, see Fig. 10. In this computation, radius of the nanowire has varied from 25 nm to 250 nm.
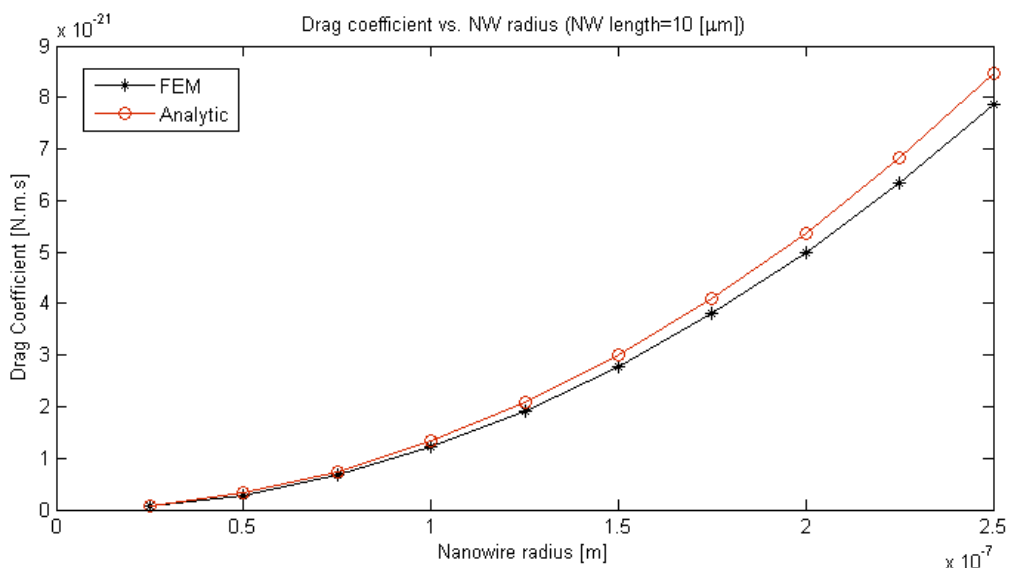
Fig. 10. The dependence of drag coefficient, i.e., ratio of torsional drag to angular velocity, on the radius of a circular nanowire. The length of the nanowire is fixed to 10 µm. Each of the data points corresponds to an individual FEM simulation 2D-COMSOL Fluid Dynamics, Laminar flow module.

## 2.5. Nanowires in Rotational Motion about its short axis

Commercial finite element analysis software packages with fluid-structure interaction capabilities can be used to solve these equations for the immersed probes with complex geometries and boundary conditions. The model is extended to calculate the hydrodynamic drag forces of the nanowires in an arbitrary motion. In the model, the constant flow velocity imposed on the inlet port introduces a force on the nanowire to rotate in the flow direction. The model is constructed to allow the rotation of the nanowire whose one end is constrained to a rotational motion around x and y axis. Note that the displacement of the constrained NW-end, i.e., the rotation axis, is taken zero in all x, y and z directions (Fig.11 (a)). Keeping in mind that the nanowire is not bended along the flow direction, only is rotated around the constrained axis in this configuration.

   In the model, dimension of the fluid domain is fixed to a square dimension with a length of 50 µm. The dimension of the cylindrical nanowire is varied with radii from 50 nm to 150 nm, and lengths from 2 µm to 10 µm. The boundaries of the computational domain in the model are defined as the inlet port with a velocity flow of 10-10m/s, the outlet ports with zero pressure. Fig. 11(b) shows the dependence of the drag coefficient on the different lengths of nanowires which are in rotational motion along the flow direction. For this computation, the nanowire diameter is fixed to 200 nm. In order to understand the results of FEM-simulations, we also analyzed an approximate analytical models presented in [22]. The sketch of the analytic model is represented in Fig. 11(a). The drag coefficient for the rotation occurs in x-y

plane when the pivot point of the rotation is shifted by a value ξ from center-of-mass is considered,

$$\frac{\tau}{\omega} = \frac{\pi\eta(L+2\xi)^3}{3(\ln p'+C')} \tag{7}$$

now $p' = (L + 2\xi)/D$ is the effective length-to-diameter ratio and C' is the effective end correction which takes into account the shift of the rotation pivot point with respect to the center-of-mass (end of the nanowire). The dependence of the drag coefficient on the nanowire which is calculated by the analytical model is shown in Fig. 11(c). In the analytical calculation, the radius of the nanowire is fixed to 100 nm.
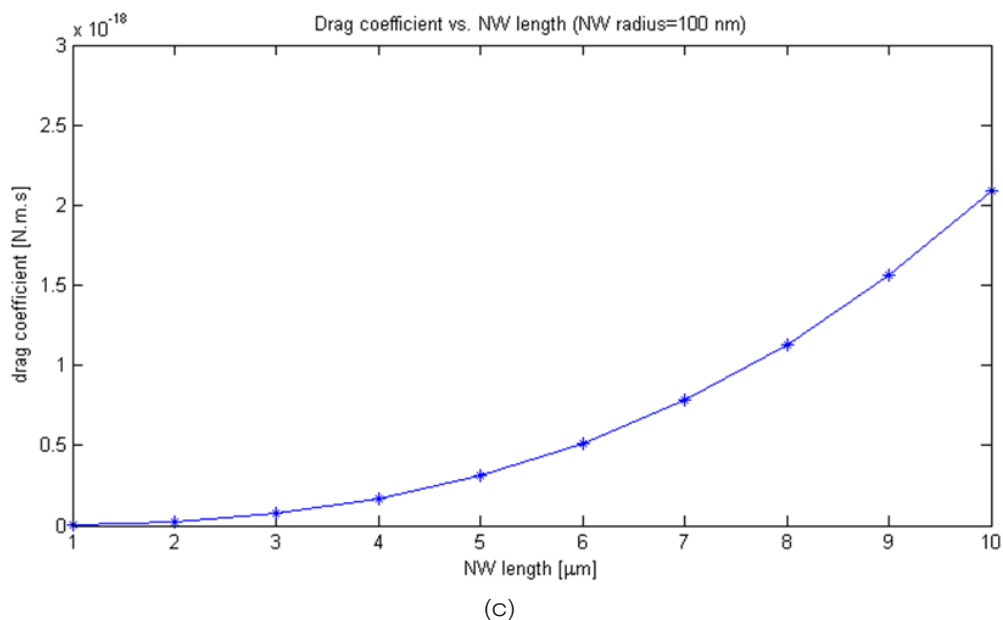

(a)

(b)

(c)
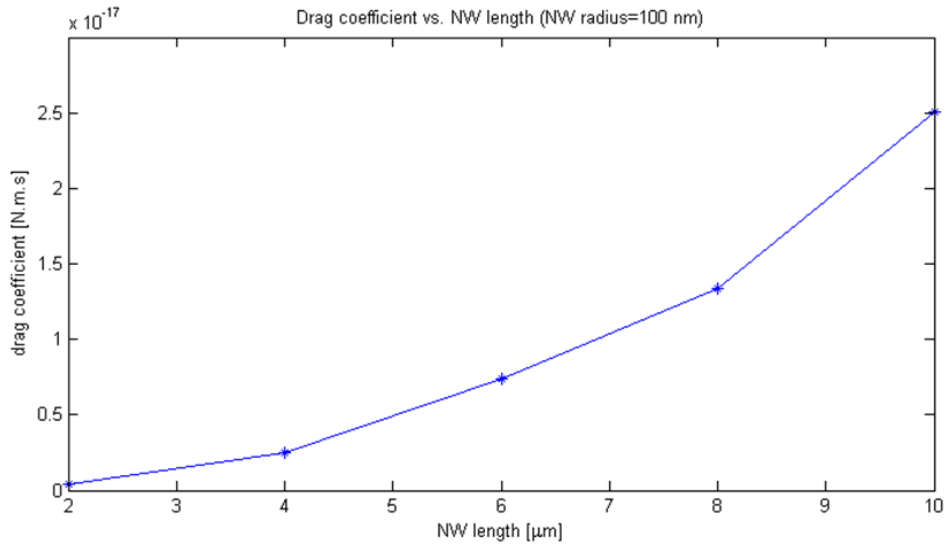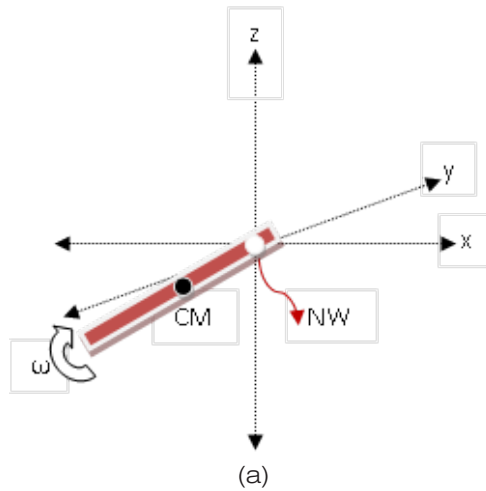
Fig. 11. Sketch of the geometric configuration for a nanowire (a) Rotation occurs in the x-y plane. (b) The dependence of drag coefficient, i.e., ratio of torsional drag to angular velocity, on the length of a circular nanowire. The diameter of the nanowire is fixed to 200 nm. Each of the data points corresponds to an individual FEM simulation (c), calculated using analytical models presented by [17,18].

3. CONCLUSION

In this paper, CFD approach has been used to investigate laminar flow caused by long cylinder translating parallel to long axis and/or rotating around its endpoint. Several numerical methods dealing with solid motion in fluid, including some CFD methods and Finite element method (FEM), have been compared. The relationship between cylinder length, cylinder diameter, translational velocity, rotation speed, wall effects and drag coefficient has been systematically researched. Finally, the conclusions are as below:

- The dependence of drag coefficient on the length and diameter of a circular nanowire is obtained in open boundary. Good agreement is observed with approximate analytical models presented by Happel & Brenner [19] and Dupont [20]. Happel & Brenner solution is based on low Reynolds hydrodynamics and valid for circular cylinders. The results were cross-checked for velocity dependence and linear dependency between force and velocity was confirmed. The model with open boundaries captures well the behavior of nanowires immersed in an infinitely large liquid domain.

- Wall effects are investigated in a in a completely enclosed chamber (microfluidic channel). There is an increase in drag coefficient when compared with the case when there are no stationary walls. The predicted drag force on a nanowire with a radius of 100 nm and a length of 10 µm that translates with a constant speed of 100 µm/s is around 1 pN and the drag force almost doubles when the nanowire is confined in a closed cylindrical liquid environment with a height of 100 µm and a radius of 250 µm.

- Hydrodynamic behavior of the nanowire in rotational motion about its long axis and its short axis is also examined. The relevant drag coefficient for a rod-like object is related to the rotation axes. When FEM simulations are also compared to an approximate analytical model, it is observed that the model captures well the drag torque changes as nanowires motion about its long axis.

REFERENCES

[1] Dayeh S. A., Aplin D. P. R., Zhou X., Yu P. K.L., Yu E.T., Wang D. (2007). "High electron mobility InAs nanowire field-effect transistors," Small, vol. 3, pp. 326-332.

[2] Stevenson C. P. T., Martensson T., Tragardh J., Larsson C., Rask M., Hessmann D., Samuelson L., Ohlsson J., (2008). "Monolithic GaAs/InGaP nanowire light emitting diodes on silicon," Nanotechnology, vol. 19.

[3] Yan Z., Pelton M., Vigderman L., Zubarev E. R., and Scherer N. F., (2013). "Why Single-Beam Optical Tweezers Trap Gold Nanowires in Three Dimensions, " ACS Nano, vol.7, No.10.

[4] Berezney J.P., Valentine M. T., (2022). " A compact rotary magnetic tweezers device for dynamic material analysis, " Review of Scientific Instruments, vol. 93, 093701.

[5] Dodampegama S., Mudugamuwa A., Konara M., Perera N., De Silva D., Roshan U., Amarasinghe R., Jayavera N. And Tamura H., (2022). " A Review on the Motion of Magnetically Actuated Bio-Inspired Microrobots, " Appl. Sci. 12(22), 11542.

[6] Zhang, W., Wen, M., Liu, P., Yang, G., & Lei, H. (2021). " Microsphere-assisted manipulation of a single Ag nanowire, " Nanophotonics, vol. 10 (10), 2729-2736.

[7] Marago, O. M., Jones, P. H., Gucciardi, P. G., Volpe, G., & Ferrari, A. C. (2013). " Optical trapping and manipulation of nanostructures, " Nature nanotechnology, vol. 8 (11), 807-819.

[8] Rawtani, D., Sajan, T., Twinkle R, A., & Agrawal, Y. K. (2015). " Emerging strategies for synthesis and manipulation of nanowires: a review, " Reviews on advanced materials science, vol. 40 (2).

[9] Bentley A. K., Jeremy S., Arthur B. E., and Crone W. C., (2004) "Magnetic manipulation of copper-tin nanowires capped with nickel ends," Nano Lett. vol. 4, pp. 487-490.

[10] Bentley A. K., Farhoud M., Arthur B. E., Nickel A. M. L., Lisensky G. C. And Crone W. C., (2005). "Template synthesis and magnetic manipulation of nickel nanowires," J. Chem. Educ. vol. 82, pp. 765- 768.

[11] [11]. Fan D. L., Zhu F. Q., Cammarata R. C., and Chien C. L., (2005). "Controllable high-speed rotation of nanowires," Phys. Rev. Lett. vol. 94.

[12] Hangarter C. M. and Myung N. V., (2005). "Magnetic alignment of nanowires," Chem. Mater. vol. 17, pp. 1320-1324.

[13] Gao C., Li W., Morimoto H., Nagaoka Y., and Maekawa T., (2006). "Magnetic carbon nanotubes: Synthesis by electrostatic selfassembly approach and application in biomanipulations," J. Phys. Chem. B vol. 110, pp. 7213-7220.

[14] Yan, R., Gargas, D., and Yang, P. (2009). "Nanowire photonics," Nature photonics, vol. 3 (10), 569-576.

[15] Yu, K., Yi, J., & Shan, J. W. (2018). "Real-time motion planning of multiple nanowires in fluid suspension under electric-field actuation. " International Journal of Intelligent Robotics and Applications, vol. 2 (4), 383-399.

[16] Mechlera Á., Piorek B., Lal R., and Banerjee S., (2004). "Nanoscale velocity–drag force relationship in thin liquid layers measured by atomic force microscopy, " Applied Physics Letters, vol. 85, Number 17 3881.

[17] H. Lamb, Hydrodynamics (Dover, New York, 1945), 6th ed., ISBN 0-486- 60256-7.

[18] K. Batchelor, An Introduction to Fluid Dynamics (Cambridge University Press, Cambridge, 1967)

[19] Brenner, H. (1961) " The slow motion of a sphere through a viscous fluid towards a plane surface. " Chem. Eng Sci., 16, 242-251.

[20] Dhont J. K., and Briels W.J., "Rod-like Brownian particles in shear flow, Soft Matter: Complex Colloidal Suspensions, " WILEY-VCH Verlag Berlin GmbH, edited by G. Gompper, and M. Schick, 2, (2006).

[21] Yan Zongyi. Low Reynolds Number Fluid Theory, (Peking University Press 2002).

[22] Neves A. A. R., Camposeo A., Pagliara S., Saija R., Borghese F., Denti P., Lati M. A., Cingolani R., Marago M. O., and Pisignano D., (2010) "Rotational dynamics of optically trapped nanofibers, " Optics Express, vol. 18. No. 2.

[23] Ghosh A., Mandal P., Karmakar S., and Ghosh A., (2013). "Analytical theory and stability analysis of an elongated nanoscale object under external torque, " Phys. Chem, vol. 15, 10817.

[24] De La Torre J. G., Bloomfield V. A., (1977). "Hydrodynamic Properties of Macromolecular Complexes I. Translation, " Biopolymers, vol. 16 (8), 1747– 1763.

[25] Tirado M. M., and De La Torre J. G., (1979). "Translational Friction Coefficients of Rigid, Symmetric Top Macromolecules. Application to circular cylinders, " Journal of Chemical Physics, 71,438613.

[26] Ferziger, J.H.; Perić, M. Computational Methods for Fluid Dynamics; (Sprigner: Berlin/Heidelberg, Germany, 1999)

[27] Wang, Q., & Wang, Z. (2022). "Quantitative Analysis of Drag Force for Task-Specific Micromachine at Low Reynolds Numbers, " Micromachines, vol. 13 (7), 1134.